Levy, R., Assulin, O., Scherf, T., Levitt, M., & Anglister, J. (1989) *Biochemistry 28*, 7168-7175.
Liu, A. Y., Robinson, R. R., Hellström, K. E., Murray, E. D., Jr., Chang, P., & Hellström, I. (1987) *Proc. Natl. Acad. Sci. U.S.A. 84*, 3439-3443.
Marquart, M., Deisenhofer, J., Huber, R., & Palm, W. (1980) *J. Mol. Biol. 141*, 369-391.
Meek, K., Jeske, D., Slaoui, M., Leo, O., Urbain, J., & Capra, J. D. (1984) *J. Exp. Med. 160*, 1070-1086.
Meyer, E. F., Clore, G. M., Gronenborn, A. M., & Hansen, H. A. S. (1988) *Biochemistry 27*, 725-730.
Novotny, J., Bruccoleri, R. E., & Saul, F. A. (1989) *Biochemistry 28*, 4735-4749.
Padlan, E. A., Silverton, E. W., Sheriff, S., Cohen, G. H., Smith-Gill, S. J., & Davies, D. R. (1989) *Proc. Natl. Acad. Sci. U.S.A. 86*, 5938-5942.
Panka, D. J., Mudgett-Hunter, M., Parks, D. R., Peterson, L. L., Herzenberg, L. A., Haber, E., & Margolies, M. N. (1988) *Proc. Natl. Acad. Sci. U.S.A. 85*, 3080-3084.
Saul, R., Amzel, L., & Poljak, R. (1978) *J. Biol. Chem. 253*, 585-597.
Segal, D., Padlan, E., Cohen, G. H., Rudikoff, S., Potter, M., & Davies, D. (1974) *Proc. Natl. Acad. Sci. U.S.A. 71*, 4298-4302.
Sheriff, S., Silverton, E. W., Padlan, E. A., Cohen, G. H., Smith-Gill, S. J., Finzel, B. C., & Davies, D. R. (1987) *Proc. Natl. Acad. Sci. U.S.A. 84*, 8075-8079.
Suh, S. W., Bhat, T. N., Navia, M. A., Cohen, G. H., Rao, D. N., Rudikoff, S., & Davies, D. (1986) *Proteins: Struct., Funct., Genet. 1*, 74-80.
Winter, E., Radbruch, A., & Krawinkel, U. (1985) *EMBO J. 4*, 2861-2867.
Wüthrich, K. (1986) *NMR of Proteins and Nucleic Acids*, Wiley, New York.
Wüthrich, K., Billeter, M., & Braun, W. (1983) *J. Mol. Biol. 169*, 949-961.

NMR Identification of Protein Surfaces Using Paramagnetic Probes

Andrew M. Petros,[‡] Luciano Mueller,[§] and Kenneth D. Kopple*
SmithKline Beecham Pharmaceuticals, P.O. Box 1539, King of Prussia, Pennsylvania 19406
Received March 16, 1990; Revised Manuscript Received June 22, 1990

ABSTRACT: Paramagnetic agents produce line broadening and thus cancellation of anti phase cross-peak components in two-dimensional correlated nuclear magnetic resonance spectra. The specificity of this effect was examined to determine its utility for identifying surface residues of proteins. Ubiquitin and hen egg white lysozyme, for which X-ray crystal structures and proton NMR assignments are available, served as test cases. Two relaxation reagents were employed, 4-hydroxy-2,2,6,6-tetramethylpiperidinyl-1-oxy and the gadolinium(III) diethylenetriaminepentaacetate complex ion. Correlations were sought between reagent-produced decreases of side-chain cross-peak volumes in double-quantum-filtered proton correlation (DQF-COSY) spectra and the solvent-exposed side-chain surface area of the corresponding residues. The lanthanide complex produced strong effects ascribable to association with carboxylate groups but was not otherwise useful in delineating surface residues. The nitroxyl, on the other hand, produced clear distinctions among the Val, Leu, and Ile residues that generally paralleled side-chain exposure in the crystal, although consistent correlations were not observed with residues of other types. Although an instance of possible specific protein-nitroxyl association was noted, the nitroxyl appears to be a tool for identifying hydrophobic surface residues.

For most enzymes and for globular proteins in general, surface residues play a critical functional and immunological role. Identification of a protein surface may therefore be of value in several ways. For hormonally active proteins, knowledge of the surface may aid in the design of peptide agonists and antagonists, especially when the functional regions are composed of residues not in a continuous sequence. For enzymes, mapping of surface residues may aid in identifying substrate or inhibitor binding sites, which in turn will facilitate inhibitor design. Furthermore, identification of surface residues may supplement NOE[1] and coupling constant data in the determination of protein structures by NMR.

Several methods have been proposed for using NMR spectroscopy to explore the surface structure of proteins and peptides. The photo-CIDNP technique has been used successfully to look at solvent-exposed aromatic side chains of several proteins (Kaptein et al., 1978; Kaptein, 1982; Stob et al., 1988). Other methods that have been employed or proposed include temperature dependence of amide proton chemical shifts (Kopple et al., 1969), proton-deuteron exchange rates (Wagner & Wuthrich, 1982), pH-rate profiles

* To whom correspondence should be addressed at SmithKline Beecham Pharmaceuticals, L-940, P.O. Box 1539, King of Prussia, PA 19406-0939.
‡ Present address: Abbott Laboratories, Dept. 47G. Bldg. AP9, Abbott Park, IL 60064.
§ Present address: Squibb Institute for Medical Research, Room D4159, P.O. Box 4000, Princeton, NJ 08543.

[1] Abbreviations: NOE, nuclear Overhauser effect; NMR, nuclear magnetic resonance; 1D, one dimensional; 2D, two dimensional; CIDNP, chemically induced dynamic nuclear polarization; COSY, correlated spectroscopy; DQF, double quantum filtered; HyTEMPO, 4-hydroxy-2,2,6,6-tetramethylpiperidinyl-1-oxy; Gd[DTPA], gadolinium(III) diethylenetriaminepentaacetate complex ion; hew, hen egg white; NOESY, nuclear Overhauser effect spectroscopy; TOCSY, totally correlated spectroscopy; tri-NAG, tri-*N*-acetylglucosamine.

0006-2960/90/0429-10041$02.50/0

(Molday et al., 1974), solvent saturation (Pitner et al., 1975), and paramagnetic broadening by soluble free radicals (Kopple & Schamper, 1972; Kopple & Zhu, 1983; Niccolai et al., 1982). This last technique, the use of spin-labels as paramagnetic probes, is the subject of this study.

The effect of free radicals and other paramagnetic species on proteins has been explored for the most part by one-dimensional NMR spectroscopy (Chazin et al., 1987; Lane & Jardetzky, 1985). One-dimensional measurements are however limited to peptides and small proteins, since spectra of larger proteins are too crowded to allow the broadening of any but a few resonances to be observed. The obvious advantage of two-dimensional spectroscopy is the greater spectral dispersion it provides. For proteins of up to 10000–15000 kDa there are still many cross-peaks which are resolved well enough in 2D spectra for quantitative intensity measurements to be made. Use of the effects of spin-labels on 2D NMR spectra was demonstrated by Kosen et al. (1986), who successfully used 2D spectroscopy to look at bovine pancreatic trypsin inhibitor which had been covalently spin-labeled at three different positions. Their absolute-value COSY data showed that cross-peaks from residues close to the spin-label were attenuated. DeJong et al. (1988) subsequently demonstrated that a spin-labeled ligand can be used to delineate a binding region by its effect on TOCSY or NOESY spectra, revealed by 2D difference spectra. For our experiments, using a spin-label as cosolute, we have employed the double-quantum-filtered phase-sensitive COSY experiment. The advantage of the COSY experiment for this purpose over, say, a NOESY or TOCSY experiment lies in the antiphase nature of the COSY cross-peaks. Since the line widths in NMR spectra of proteins are usually comparable to the coupling constants, a small amount of broadening can result in a significant amount of multiplet cancellation (Weiss et al., 1984).

As one model system we chose ubiquitin, a 76 amino acid protein which occurs throughout the plant and animal kingdoms. Although the exact physiological function of ubiquitin is not known, there is evidence that it may play a role in cytoplasmic degradation of certain target proteins. The NMR spectrum of ubiquitin has been almost completely assigned via both sequential and main chain directed methods (Weber et al., 1987; DiStephano & Wand, 1987). Furthermore, the X-ray structure of ubiquitin has been determined to 1.8-Å resolution (Vijay-Kumar et al., 1987), and this matches closely the structure in solution (P. L. Weber, personal communication). Less completely, we also examined hen egg white lysozyme and its interaction with the inhibitor tri-*N*-acetylglucosamine (tri-NAG). The proton NMR spectrum of lysozyme has been almost completely assigned (Redfield & Dobson, 1988), and crystal structures of lysozyme and lysozyme complexed with tri-NAG have been determined (Blake et al., 1965; Phillips, 1967).

Two paramagnetic agents were employed. 4-Hydroxy-2,2,6,6-tetramethylpiperidinyl-*N*-oxy (HyTEMPO) is an organic free radical with one unpaired electron. Although nitroxyls do produce significant contact and/or pseudocontact shifts on tight complexation, e.g., hydrogen bonding in CCl_4 or $CHCl_3$ solution (Morishima et al., 1975), in the absence of tight complex formation, as in a polar solvent environment, they do not give rise to chemical shifts large enough to hinder comparison of complex 2D spectra. Gadolinium diethylenetriaminepentaacetate complex ion (Gd[DTPA]) is an octacoordinate complex of Gd^{3+} and the diethylenetriaminepentaacetic acid moiety. The complex has a net charge of −2 and a very high association constant, ca. 10^{23}. Gadolinium ion is a pure relaxation probe. Both reagents were employed with ubiquitin; only the nitroxyl was used in the lysozyme study.

Materials and Methods

Ubiquitin, hew lysozyme, and tri-*N*-acetylglucosamine (*N*,*N*′,*N*″-triacetylchitotriose) were purchased from Sigma Chemical Co. Deuterium oxide and acetic acid-d_4 were obtained from Merck, Sharp and Dohme, and HyTEMPO was obtained from Aldrich. Gd[DTPA] was prepared via a minor modification of previously published procedures (R. Rycyna, personal communication; Marsh, 1955; Rubin & Dexter, 1962). Protein spectra were obtained at the same temperatures and pH used for the published assignments. NMR samples of ubiquitin (~5 mM) were prepared in 100% deuterium oxide and 25 mM acetic acid-d_4, and the pH was adjusted to 4.7 (direct pH meter reading at room temperature). Lysozyme samples (~5 mM) were prepared in the same way except the pH was adjusted to 3.8. HyTEMPO, Gd[DPTA], and tri-NAG were added to the protein samples as microliter volumes of concentrated D_2O solutions.

NMR experiments were carried out at 500 MHz on a JEOL GX-500 spectrometer, under conditions matching those for which the NMR assignments were made. Data were transferred to a MicroVAX II for processing with FT NMR software (Hare Research Inc., Woodinville, WA). DQF-COSY experiments were performed followed standard procedures (Piantini et al., 1982; Shaka & Freeman, 1983), and quadrature detection in ω_1 was obtained by the hypercomplex method (States et al., 1982). Ubiquitin spectra were collected at 50 °C, and suppression of the residual HDO signal was carried out by continuous irradiation with weak power during the relaxation delay, 1.7 s. A total of 400 t_1 spectra were collected per experiment, 2K data points each, with 16 transients per spectrum. Data sets were 2K × 2K zero-filled matrices processed with a skewed–shifted (30°) sine bell in both dimensions. Lysozyme spectra were recorded and processed in the same way, but the probe temperature was maintained at 35 °C.

Integrated COSY cross-peak volumes were calculated by using the FT NMR software, and the ratio (V/V_0) of cross-peak volume in the presence of paramagnetic agent to the volume in its absence was determined. For nonoverlapping cross-peaks produced by diastereotopic pairs, as in Val or Leu $CH(CH_3)_2$ or Ile CH_2CH_3 units, the average value of V/V_0 was calculated. In some instances, however, measurement of both peaks was precluded by overlap with other resonances. Those exceptions are indicated in the tabulated results.

The accessible surface areas for specific proton groups of ubiquitin and hen egg white lysozyme were calculated from crystal structures by using the Connolly molecular surface program (Connolly, 1981; Quantum Chemistry Program Exchange, Department of Chemistry, Indiana University). For ubiquitin two different radii were used, 2.5 and 4.5 Å, taken from models to represent effective radii for HyTEMPO and Gd[DTPA], respectively. Only the 2.5-Å value was used for lysozyme. Protein Data Bank files for ubiquitin (Vijay-Kumar et al., 1987) and lysozyme (Diamond, 1974) were used as input for the surface program. The default van der Waals radii of the Connolly program, which are chosen to produce a united atom approximation to include hydrogens, were used. The areas calculated were of the groups producing the cross-peaks examined, not of entire side chains. For example, the surface area calculated for the $C^{\gamma 1}H_2$–$C^{\delta}H_3$ cross-peaks of Ile 3 was the area of the γ1-methylene group plus the area of the δ-methyl group. Since stereospecific assignments of the dia-

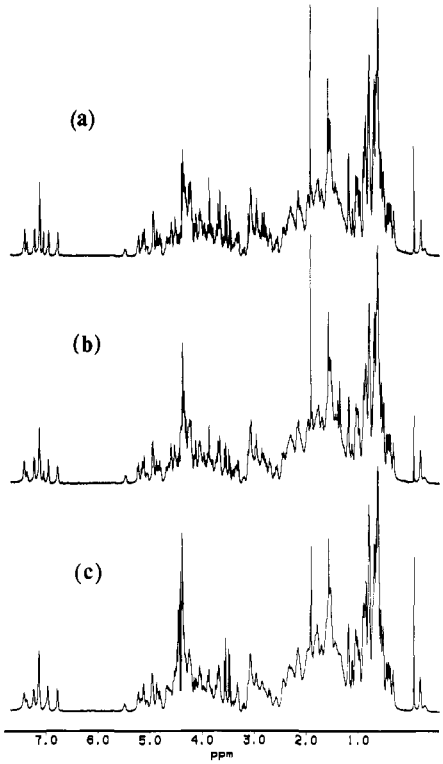

FIGURE 1: Effect of HyTEMPO and Gd[DTPA] on the 1D spectrum of ubiquitin: (a) no paramagnetic reagent; (b) 20 mM HyTEMPO; (c) 1 mM Gd[DTPA].

stereotopic methylene protons are not available, no attempt was made to treat these or other diastereotopic pairs separately. The density of dots used in the Connolly representation of the surface was 20 dots/Å^2, and surface areas in Å^2 were obtained by counting dots.

Results and Discussion

Ubiquitin. Figure 1 shows one-dimensional spectra of ubiquitin (a) with no paramagnetic reagent present, (b) in the presence of 20 mM HyTEMPO, and (c) in the presence of 1 mM Gd[DTPA]. the two paramagnetic reagents cause relatively slight overall broadening of the ubiquitin resonances at these concentrations. It is possible to observe some differential effects in the relatively uncrowded aromatic region of these spectra. The width of half-height of a His resonance at 7.15 ppm is observed to broaden from 5 to 19 Hz on addition of HyTEMPO and from 5 to about 24 Hz on addition of Gd[DTPA], while the other aromatic resonances are broadened by a few hertz at most. To observe differential effects in the aliphatic region, however, it is necessary to turn to two-dimensional spectra.

Figures 2 and 3 are expansions from the upfield regions of ubiquitin DQF-COSY spectra containing CH–CH$_3$ cross-peaks of Ile, Leu, and Val. Figure 2 shows peaks arising from Ile 3, 13, 36 and 44. It can be seen that 20 mM HyTEMPO completely eliminates the peaks from Ile 36 and 44, leaving those from Ile 3 and 13 visibly unaffected. Exploratory experiments had indicated that such distinctions were clearest at that radical concentration. Addition of 1.0 mM Gd[DTPA] broadens but does not eliminate the Ile 36 and 44 peaks. In Figure 3 are expansions containing cross-peaks from Leu 8, Ile 13, Ile 30, and Val 70. Examination shows that the peaks from Leu 8 and Val 70 are strongly affected by both HyTEMPO and GD[DTPA] while those from Ile 13 and Ile 30 are unaffected. The hypothesis that arises from these observations is that the side chains with resonances affected by

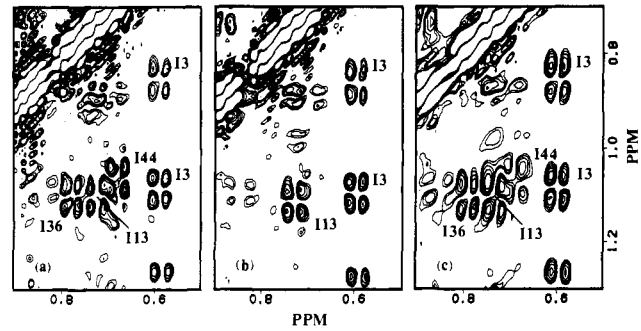

FIGURE 2: Effect of HyTEMPO and Gd[DTPA] on isoleucine side chains: shown are C$^{\gamma 1}$H–C$^{\delta}$H$_3$ cross-peaks for I3, I13, I36, and I44. (a) No paramagnetic agent; (b) 20 mM HyTEMPO; (c) 1 mM Gd[DTPA].

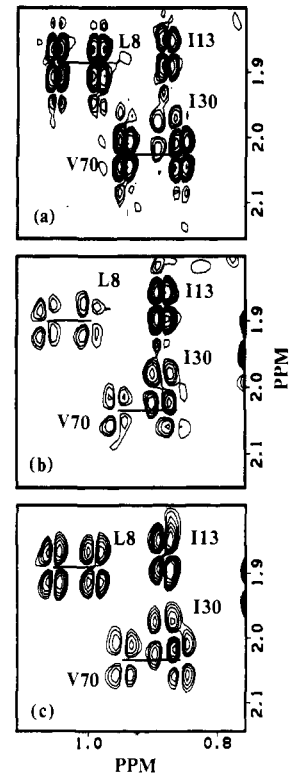

FIGURE 3: Effect of HyTEMPO and Gd[DTPA] on isoleucine, valine, and isoleucine side chains: shown are C$^{\gamma}$H–C$^{\delta}$H$_3$ cross-peaks for L8, C$^{\beta}$H–C$^{\gamma}$H$_3$ cross-peaks for V70, C$^{\beta}$H–C$^{\gamma 2}$H$_3$ cross-peaks for I30, and a C$^{\gamma 1}$H–C$^{\delta}$H$_3$ cross-peak for I13. (a) No paramagnetic reagent; (b) 20 mM HyTEMPO; (c) 1 mM Gd[DTPA].

the paramagnetic reagents, i.e., of Ile 36, Ile 44, Leu 8, and Val 70, are on the surface of the protein, in contact with solvent and the paramagnetic reagent, while the side chains that are not affected by the reagents are buried. To obtain a quantitative estimate of the effect of the paramagnetic reagents on the DQF-COSY cross-peaks, we measured the ratio of cross-peak volume in the presence of paramagnetic reagent (V) to the cross-peak volume in the absence of reagent (V_0). A value for V/V_0 of 0.6 was taken to be sufficiently outside error to be an arbitrary dividing line between clearly exposed and at least partially buried. More quantitative analysis in many instances would be difficult, since the extent of cancellation produced by line broadening will be dependent on the coupling constants involved. For a given residue type we have compared cross-peaks arising from the same proton group, chosen to be as far from the backbone as possible. For Ile we monitored C$^{\gamma 1}$H–C$^{\delta}$H$_3$ cross-peaks. We also calculated the exposed surface area for these proton groups in the crystal structure of ubiquitin. Table I gives the volumes of the

Table I: Effect of Paramagnetic Reagents on Ubiquitin Side-Chain Resonances

residue	cross-peak type	V/V_0[a] Hy-TEMPO	V/V_0[a] Gd[DTPA]	surface area (Å²)[b] r = 2.5	surface area (Å²)[b] r = 4.5	residue	cross-peak type	V/V_0[a] Hy-TEMPO	V/V_0[a] Gd[DTPA]	surface area (Å²)[b] r = 2.5	surface area (Å²)[b] r = 4.5
I3	$C^{\gamma 1}H$–$C^{\delta}H_3$	1	0.9	0	0	T7	$C^{\beta}H$–$C^{\gamma}H_3$	<0.1	0.6	0	0
I13	$C^{\gamma 1}H$–$C^{\delta}H_3$*	0.8	1	0	0	T9	$C^{\beta}H$–$C^{\gamma}H_3$	0.3	0.4	15.4	9.6
I23	$C^{\gamma 1}H$–$C^{\delta}H_3$	0.9	0.8	0	0	T12	$C^{\beta}H$–$C^{\gamma}H_3$	0.6	0.4	3.5	1.2
I30	$C^{\gamma 1}H$–$C^{\delta}H_3$	0.9	1	0	0	T14	$C^{\beta}H$–$C^{\gamma}H_3$	0.9	0.6	5.1	2.8
I36	$C^{\gamma 1}H$–$C^{\delta}H_3$*	<0.1	0.8	2.9	0.4	T22	$C^{\beta}H$–$C^{\gamma}H_3$	0.9	0.5	7.2	3.8
I44	$C^{\gamma 1}H$–$C^{\delta}H_3$	<0.1	0.5	2.4	0	T55	$C^{\beta}H$–$C^{\gamma}H_3$	1	0.1	4.8	2.1
I61	$C^{\gamma 1}H$–$C^{\delta}H_3$	1	0.8	0	0	T66	$C^{\beta}H$–$C^{\gamma}H_3$	0.9	<0.1	2.2	0.8
L8	$C^{\gamma}H$–$C^{\delta}H_3$	0.3	0.3	17.3	9.5	F4	$C^{\delta}H$–$C^{\epsilon}H$	0.9	0.8	5.9	2.9
L15	$C^{\gamma}H$–$C^{\delta}H_3$*	1	1	0	0	F45	$C^{\delta}H$–$C^{\epsilon}H$	0.9	0.4	2.5	0.7
L43	$C^{\gamma}H$–$C^{\delta}H_3$	0.9	0.7	0	0	Y59	$C^{\delta}H$–$C^{\epsilon}H$	0.3	0.8	2.1	0.4
L50	$C^{\gamma}H$–$C^{\delta}H_3$	0.8	0.9	0	0	H68	$C^{\alpha}H$–$C^{\beta}H$	0.4	0.4	0.2	0
L56	$C^{\gamma}H$–$C^{\delta}H_3$	1	0.9	0	0	D21[c]	$C^{\alpha}H$–$C^{\beta}H$	1	<0.1	0 (4.6)	0 (2.2)
L67	$C^{\gamma}H$–$C^{\delta}H_3$	1	0.9	0	0	D32	$C^{\alpha}H$–$C^{\beta}H$	0.6	<0.1	0.2 (22.4)	0 (13.9)
L69	$C^{\gamma}H$–$C^{\delta}H_3$	0.6	1	0	0	D39	$C^{\alpha}H$–$C^{\beta}H$	0.6	<0.1	7.4 (12.4)	3.2 (5.2)
L71	$C^{\gamma}H$–$C^{\delta}H_3$	0.5	0.5	3.4	0.5	D52	$C^{\alpha}H$–$C^{\beta}H$	0.6	0.1	2.3 (8.8)	0.6 (2.5)
L73	$C^{\gamma}H$–$C^{\delta}H_3$	0.5	0.4	16.7	9.6	D58	$C^{\alpha}H$–$C^{\beta}H$	0.9	0.6	0.5 (8.6)	0 (4.9)
V5	$C^{\beta}H$–$C^{\gamma}H_3$	1	0.8	0	0	N25[d]	$C^{\alpha}H$–$C^{\beta}H$	0.5	0.2	1.2 (8.7)	0.2 (4.0)
V17	$C^{\beta}H$–$C^{\gamma}H_3$*	1	0.5	0	0	N60	$C^{\alpha}H$–$C^{\beta}H$	0.6	<0.1	3.5 (21.7)	0.9 (12.2)
V26	$C^{\beta}H$–$C^{\gamma}H_3$*	1	0.7	0	0	K6	$C^{\delta}H_2$–$C^{\epsilon}H_2$	0.7	<0.1	5.0	0.9
V70	$C^{\beta}H$–$C^{\gamma}H_3$	0.3	0.3	4.4	1.1	K11	$C^{\delta}H_2$–$C^{\epsilon}H_2$	0.6	0.3	9.7	6.5
G10	$C^{\alpha}H$–$C^{\alpha}H$	0.7	0.2	4.8	2.4	K27	not observed				
G35	$C^{\alpha}H$–$C^{\alpha}H$	0.8	0.9	4.9	3.1	K29	not observed				
G47	$C^{\alpha}H$–$C^{\alpha}H$	0.2	0.2	6.6	4.6	K33	not observed				
G53	$C^{\alpha}H$–$C^{\alpha}H$	0.8	0.4	4.4	1.8	K48	not observed				
G75	not observed					K63	$C^{\delta}H_2$–$C^{\epsilon}H_2$	0.9	0.4	13.0	8.4
G76	not observed					R42	not observed				
S20	$C^{\alpha}H$–$C^{\beta}H$	0.5	<0.1	9.7	6.7	R54	not observed				
S57	$C^{\alpha}H$–$C^{\beta}H$	0.5	0.6	5.1	2.9	R72	$C^{\gamma}H_2$–$C^{\delta}H_2$	0.6	0.5	4.9	2.0
S65	$C^{\alpha}H$–$C^{\beta}H$	0.9	0.5	1.3	0.5	R74	$C^{\gamma}H_2$–$C^{\delta}H_2$	0.7	0.5	9.6	5.4
A28	$C^{\alpha}H$–$C^{\beta}H_3$	0.8	0.2	7.2	2.6						
A46	$C^{\alpha}H$–$C^{\beta}H_3$	0.7	<0.1	9.8	3.6						

[a] V/V_0 is the ratio of the integrated cross-peak volume in the presence of the paramagnetic reagent to that in its absence. Where there are two nonoverlapping cross-peaks of the type indicated, e.g., from the Val or Leu $CH(CH_3)_2$, Ile CH_2CH_3, or Asx $CHCH_2$ units, the mean value of V/V_0 is given. As asterisk indicates that measuring both peaks was precluded by overlap with other resonances and the value of V/V_0 is for a single cross-peak. [b] r is the probe radius used in the Connolly surface program. Surface areas given are for the complete unit, e.g., $-CH(CH_3)_2$, $-CH_2CH_3$, or $-CH_2CH_2-$; diastereotopic groups are not separated. [c] For Asp and Asn side chains, the surface area values given in parentheses are for the $C^{\alpha}H$–$C^{\beta}H_2$–COO^- and $C^{\alpha}H$–$C^{\beta}H_2$–$CONH_2$ units, respectively. [d] Measured at 25 °C.

cross-peaks examined and the areas of the coupled proton groups exposed to 2.5- and 4.5-Å radius probes.

The observed relaxation of the hydrophobic side chains of Ile, Leu, and Val by HyTEMPO correlates in general with the ubiquitin crystal structure, although a quantitative relation between exposed surface area and loss of cross-peak intensity is not found. The two Ile side chains with $V/V_0 \leq 0.6$, 36 and Ile 44, are the only Ile $C^{\gamma 1}H$–$C^{\delta}H_3$ units in the crystal structure with any area exposed to a 2.5-Å radius probe. Similarly, the coupled $CHCH_3$ proton groups of Leu 8, 69, 71, and 73 and Val 70 are sensitive to the nitroxyl, and with the exception of L69, these are also the only Leu or Val $CH(CH_3)_2$ units with any surface exposed to the probe. The Leu 69 $CH(CH_3)_2$ group has no exposed surface in the crystal structure; it is shielded from the exterior by an overlying type I β-turn, T7-L8-T9-G10. However, the main-chain atoms in that turn have some of the largest temperature factors in the crystal structure (Vijay-Kumar et al., 1987), and the region is also not well-defined in solution by nuclear Overhauser effects (Weber, personal communication). Mobility of this region may allow access of radical to the Leu 69 side chain, but an alternative rationale appears below.

Two of the residues exposed to HyTEMPO, Ile 36 and Leu 69, are not exposed by our criterion to Gd[DTPA]. One reason may be that Gd[DTPA] is larger than HyTEMPO and may not have access to so much of the protein surface. In addition, the solvation requirement of the change (−2) on the complex ion may specifically hinder its approach to hydrophobic regions of the protein surface. In contrast, Val 17 is broadened by Gd[DTPA] but not by HyTEMPO. This may be a consequence of its location between Glu 16 and Glu 18, the carboxylate groups of which may, by coordination, ensure a higher average local concentration of the complex ion. The behavior of the Asp and Asn resonances, described next, strongly indicates that this is likely.

Figure 4 shows expansions of the DQF-COSY spectra containing aspartic acid and asparagine $C^{\alpha}H$–$C^{\beta}H$ cross-peaks. The Asx resonances are much more sensitive to Gd[DTPA] than those of Ile, Leu, and Val. Figure 4 shows that 0.25 mM Gd[DTPA] eliminates entirely, $V/V_0 < 0.1$, the cross-peaks of Asp 21, 32, and 39 and Asn 60. The nitroxyl-sensitive hydrophobic side chains are much less affected at this concentration of Gd[DTPA], V/V_0 = 0.5–0.8. (Cross-peak volume data in Table I are for 1.0 mM Gd[DTPA].) This difference in sensitivity between Asx and the hydrophobic residues suggests that Gd[DTPA], like lanthanide NMR reagents with chelating ligands of lower valence, coordinates with nucleophilic oxygen. Lanthanide–DTPA complexes are in fact 9-coordinate, bearing 8 ligands from the DTPA moiety plus 1 water molecule (Jenkins & Lauffer, 1988; Stezowski & Hoard, 1984). Coordination of side-chain carbonyl oxygen at the ninth site should provide more efficient relaxation of nearby protons than if the side chain approached only the outer sphere of the Gd[DTPA] ion. In the crystal, the carboxylate groups of the two Asp side chains least affected by Gd[DTPA], Asp 52 and 58, are involved in a salt bridge (to Lys 27) and

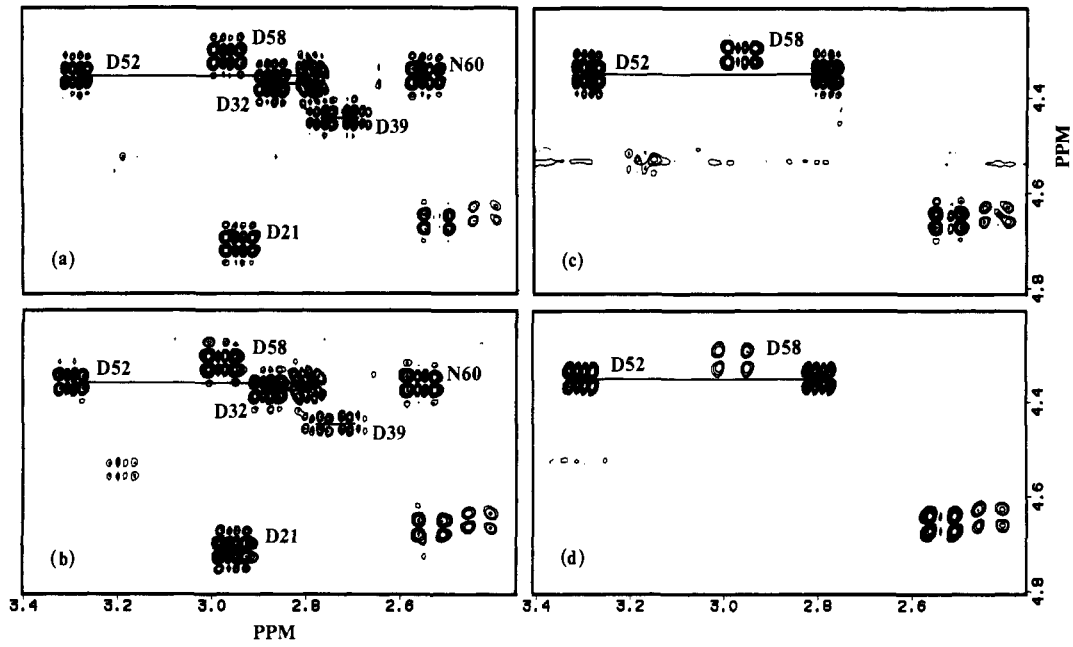

FIGURE 4: Effect of HyTEMPO and Gd[DTPA] on aspartic acid and asparagine side chains: shown are $C^{\alpha}H-C^{\beta}H_2$ cross-peaks for D21, D32, D39, D52, D58, N25, and N60. (a) No paramagnetic reagent; (b) 20 mM HyTEMPO; (c) 0.25 mM Gd[DTPA]; (d) 1 mM Gd[DTPA].

hydrogen bond (to the NH of Thr 55), respectively. These interactions would be expected to make coordination with gadolinium less favorable.

For Val, Leu, and Ile then, exposed surface in the crystal structure correlates with significant loss of cross-peak intensity when HyTEMPO is added to the ubiquitin solution, and for Asx (and presumably Glx) there is specific sensitivity to Gd[DTPA]. Further light on the behavior of the two relaxation reagents is obtained from their effects on the Lys and Arg side chains. Figure 5 shows the effects on the Lys 6, 11, and 63 $C^{\delta}H_2-C^{\epsilon}H_2$ and Arg 72 and 74 $C^{\gamma}H_2-C^{\delta}H_2$ cross-peaks. Although all of these side-chain groups have exposed surface in the crystal, it is clear from Figure 5 and Table I that HyTEMPO produces only borderline effects relative to its effects on exposed hydrophobic residues, this suggests that HyTEMPO is at least partially excluded from the solvation shells of charged or polar side chains. Although it is negatively charged, Gd[DTPA], which cannot coordinate with ammonium or guanidinium ions, does not in general affect those positively charged side chains strongly as it does most of the Asx side chains, which supports the hypothesis that Gd[DTPA] coordination products specific effects.

The correlation between exposed surface and sensitivity to nitroxyl is not so clear-cut for any of the other residues examined as it is for Val, Leu, and Ile. Although there are very definite distinctions in sensitivity among residues of a given type, their interpretations are not obvious. Figure 6 shows the region of the DQF-COSY spectrum of ubiquitin in which lie the Gly and Ser cross-peaks. The Ser 20 and 57 $C^{\alpha}H-C^{\beta}H$ and the Gly 47 $C^{\alpha}H-C^{\alpha}H$ cross-peaks are clearly affected by HyTEMPO, while the Ser 65 and Gly 10, 35, and 53 cross-peaks are unaffected or only marginally affected. Nitroxyl-insensitive Ser 65 is the least exposed of the serines in the crystal and nitroxyl-sensitive Gly 47 is the most exposed of the glycines, but the coupled proton groups of all of the Ser and Gly residues have some exposed surface.

Similarly, there is no clear correlation between exposure in the crystal and sensitivity to nitroxyl for the alanine and threonine residues (data in Table I). The $C^{\beta}H-C^{\gamma}H_3$ of Thr 9 is highly exposed in the crystal and sensitive to nitroxyl, but although the corresponding group of Thr 7 has no exposed

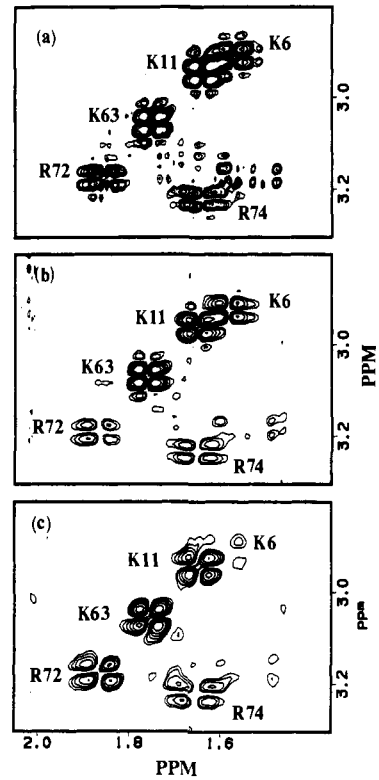

FIGURE 5: Effect of HyTEMPO and Gd[DTPA] on lysine and arginine side chains: shown are $C^{\delta}H_2-C^{\epsilon}H_2$ cross-peaks for K6, K11, and K63 and $C^{\gamma}H_2-C^{\delta}H_2$ cross-peaks for R72 and R74. (a) No paramagnetic reagent; (b) 20 mM HyTEMPO; (c) 1 mM Gd[DTPA].

surface area in the crystal, it is even more sensitive to HyTEMPO. The spatial proximity of Thr 7 and Leu 69, both sensitive to nitroxyl and neither with exposed protons in the crystal, suggests that they might form part of a preferential site for association with HyTEMPO (see Figure 7).

The most notably sensitive of the Ser, Thr, and Ala residues to Gd[DTPA] are Ser 20, Thr 55 and 66, and Ala 46. For one of these instances the crystal structure provides an obvious explanation involving coordination of Gd[DTPA]. Ser 20 is the $i + 2$ residue of a turn, and the adjacent $i + 3$ residue is

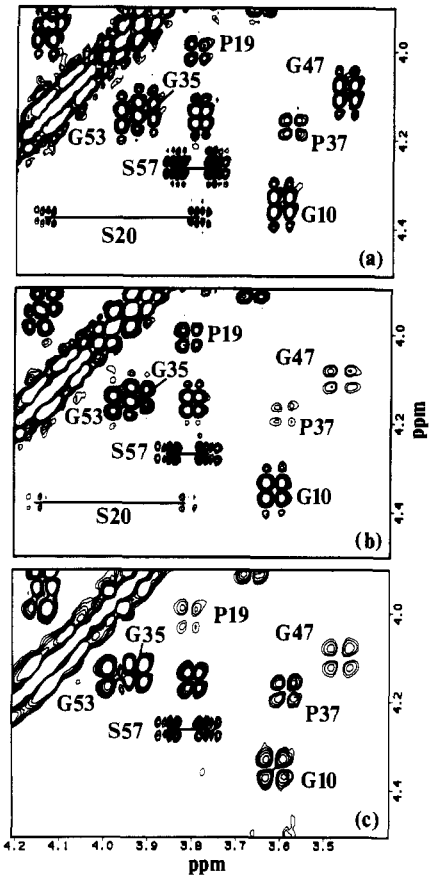

FIGURE 6: Effect of HyTEMPO and Gd[DTPA] on glycine and serine side chains: shown are $C^{\alpha}H$–$C^{\alpha}H$ cross-peaks for G10, G35, G47, and G53, $C^{\alpha}H$–$C^{\beta}H_2$ cross-peaks for S20 and S57, and $C^{\delta 1}1H$–$C^{\delta 2}H$ cross-peaks for P19 and P37. (a) No paramagnetic reagent; (b) 20 mM HyTEMPO; (c) 1 mM Gd[DTPA].

Asp 21, also extremely sensitive, which presumably coordinates with the Gd complex. Similar explanations for the others are not obvious; ad hoc explanations including changes in side-chain position and coordination to backbone carbonyls may be possible, but would not yield predictive generalizations.

Because of the potential for specific binding by coordination we do not consider that Gd[DTPA] or related molecules will be useful in general for mapping protein surfaces. However, Gd-based relaxation reagents might in some instances be useful for identifying, by elimination, some Asx $C^{\alpha}H$–$C^{\beta}H$ cross-peaks in crowded protein spectra.

On the other hand, the experiments with ubiquitin do suggest that line broadening by HyTEMPO (and presumably similar nitroxyl radicals) can be used to identify surface hydrophobic residues, although in view of the probable mobility of the surface residues and the possibility of specific association as tentatively suggested above for the Thr 7–Leu 69 region, the correlation with a crystal structure may not be perfect. A stereoview of ubiquitin showing Val, Leu, and Ile residues (Figure 7) shows a striking distinction between nitroxyl-sensitive and nitroxyl-insensitive residues. The insensitive residues are inside the ubiquitin barrel, and the sensitive residues are at the top, bottom, or side. In view of the relative rarity of surface hydrophobic residues, the ability to identify them (and the linearly adjacent residues by nuclear Overhauser effects) in advance of a complete structure could be useful in providing indications of chain folding or clues to functional portions of a protein surface.

Hen Egg White Lysozyme. The binding pocket of hen egg white lysozyme contains a high proportion of hydrophobic residues. Therefore, we used it to examine further the utility of HyTEMPO for mapping exposed protein surface and ligand binding to the surface.

Table II: Effect of HyTEMPO on Lysozyme Side Chains

residue	cross-peak type	V/V_0[a]	accessible area[b] (Å^2)
Asp 52	$C^{\alpha}H$–$C^{\beta}H$	1.0	0.4
Leu 56	$C^{\gamma}H$–$C^{\delta}H_3$	1.0	0.0
Ile 58	$C^{\beta}H$–$C^{\gamma 2}H_3$	0.9	0.0
Asn 59	$C^{\alpha}H$–$C^{\beta}H$	<0.1	1.7
Trp 62	$C^{4}H$–$C^{5}H$	<0.1	5.2
Trp 63	$C^{4}H$–$C^{5}H$	<0.1	2.4
Leu 75*	$C^{\gamma}H$–$C^{\delta}H_3$	<0.1	13.0
Ile 98	$C^{\beta}H$–$C^{\gamma 2}H_3$	<0.1	0.0
Val 99	$C^{\beta}H$–$C^{\gamma}H_3$	1.0	0.0
Asp 101	$C^{\alpha}H$–$C^{\beta}H$	<0.1	5.3
Gly 102	$C^{\alpha}H$–$C^{\alpha}H$	<0.1	3.1
Ala 107	$C^{\alpha}H$–$C^{\beta}H_3$	<0.1	1.2
Trp 108	$C^{4}H$–$C^{5}H$	0.9	0.0
Val 109*	$C^{\beta}H$–$C^{\gamma}H_3$	0.6	12.7

[a] V/V_0 is the ratio of the integrated cross-peak volume in the presence of the paramagnetic reagent to that in its absence. Where there are two nonoverlapping cross-peaks of the type indicated, e.g., for the Val or Leu $CH(CH_3)_2$ or Asx $CHCH_2$ units, the mean value of V/V_0 is given. An asterisk indicates that measuring both peaks was precluded by overlap with other resonances and the value of V/V_0 is for a single cross-peak. [b] Probe radius 2.5 Å. Stereospecific assignments of diastereotopic groups are not available. The surface areas given are for the complete unit, e.g., $-CH(CH_3)_2$ or $-CHCH_2-$.

Clear differential broadening effects for lysozyme occurred at a lower concentration of HyTEMPO, 10 mM, than for ubiquitin, 20 mM. For the paramagnetic perturbations involved, T_2(dipolar) is inversely proportional to rotational correlation time (Kemple et al., 1988). Since lysozyme, 14.6 kDa, should have a longer rotational correlation time than ubiquitin, 8.6 kDa, this observation suggests that the effects of HyTEMPO are produced not solely by collision, for which the effective correlation time would be comparable to that of HyTEMPO in solution, but to some extent by an association that persists for a period at least of the order of the longer protein rotational correlation time.

Figure 8 shows expansions from the upfield region of lysozyme DQF-COSY spectra containing CH–CH_3 cross-peaks of Ile, Leu, and Val. By comparison of panels a and b, it can be seen that 10 mM HyTEMPO eliminates the cross-peak for Leu 75, leaving the others effectively unchanged. The surface area of the C^{γ} and two C^{δ} groups of Leu 75 exposed to a 2.5-Å probe was calculated to be 13 Å^2. In contrast, of the groups giving rise to the resonances that are unchanged, the C^{β} and C^{γ} groups of Val 92, the C^{β} and $C^{\gamma 2}$ groups of Ile 55 and Ile 88, and the C^{γ} and C^{δ} groups of Leu 8, Leu 83, and Leu 129 are all calculated to have zero accessibility.

Figure 9 shows analogously some Ala $C^{\alpha}H$–$C^{\beta}H_3$ and Thr $C^{\beta}H$–$C^{\gamma}H_3$ cross-peaks of lysozyme. Panels a and b show that the cross-peaks for Ala 122 and Ala 107 are removed by nitroxyl and that for Ala 31 is unaffected. The C^{α} plus C^{β} accessibilities for 107 and 122 are 1.2 and 3.4 Å^2, respectively. For Ala 31, there is no exposed surface. Although the correlation appears to hold for the 3 Ala residues in the figure, data were not obtained for all 12 Ala residues. There is no correlation for the 3 Thr residues in the figure. None of the Thr $C^{\beta}H$–$C^{\gamma}H_2$ cross-peaks is strongly affected by nitroxyl, yet all have some calculated accessibility. The C^{β} plus C^{γ} accessibilities to the 2.5-Å probe are 1.5 Å^2 for Thr 43, 8.7 Å^2 for Thr 89, and 7.8 Å^2 for Thr 118.

Table II compares the V/V_0 ratio for DQF-COSY cross-peaks of a number of additional residues, those in the vicinity of the binding site, with the accessibility of the corresponding atomic groups to the 2.5-Å probe. The agreement here between the relaxation result and the calculated exposure is good

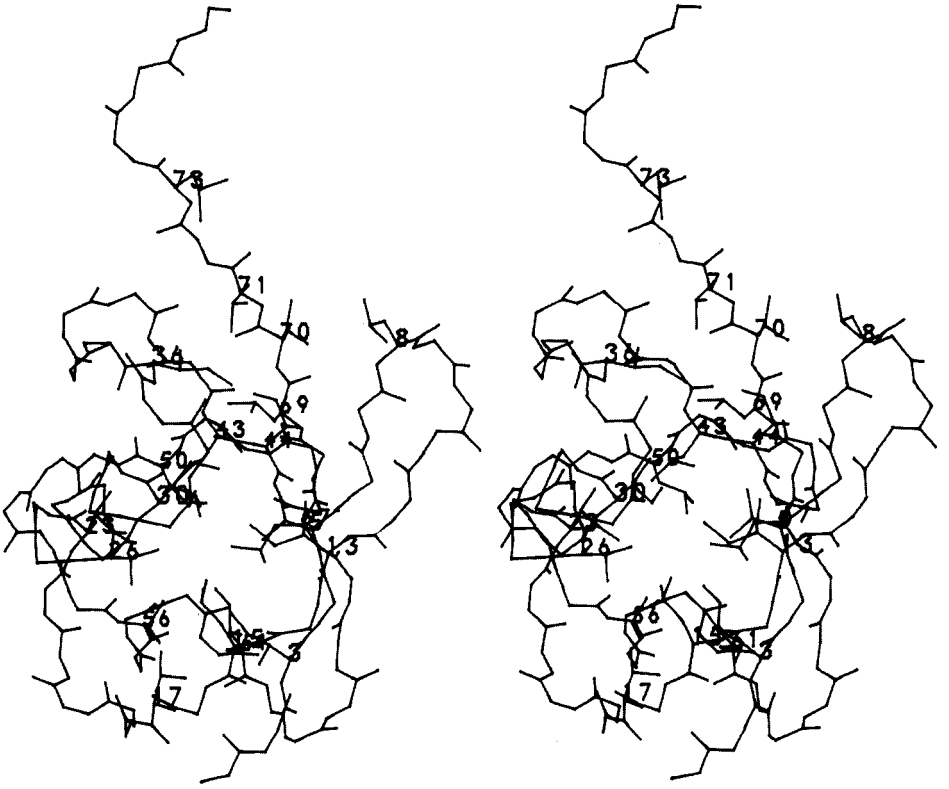

FIGURE 7: Stereoview of the ubiquitin backbone in the crystal (Vijay-Kumar et al., 1987). Side chains and numbering of the Val, Leu, and Ile residues are indicated. Nitroxyl-sensitive residues are 8, 36, 44, 69, 70, 71, and 73. (See Table I). The possible nitroxyl binding region between Leu 69 and Thr 7 suggested in the text is visible in this view. The figure was generated at Abbott Laboratories with software written there.

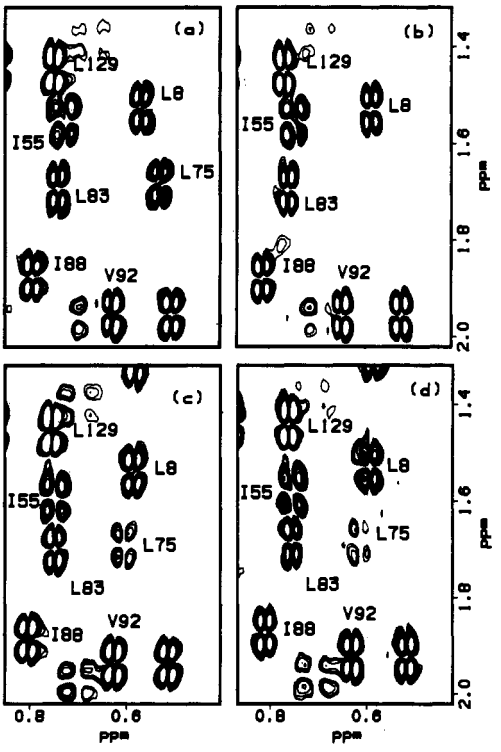

FIGURE 8: Effect of HyTEMPO on some Ile, Leu, and Val side-chain cross-peaks of lysozyme in the absence and presence of tri-NAG. (a) Lysozyme. (b) Same as (a) with 10 mM HyTEMPO added. (c) Same as (a) with 10 mM tri-NAG added. (d) Same as (a) with 10 mM tri-NAG and 10 mM HyTEMPO added.

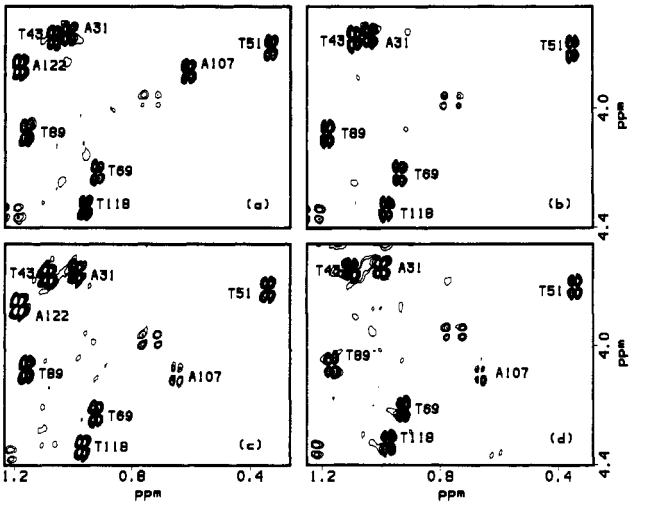

FIGURE 9: Effect of HyTEMPO on Ala and Thr side-chain resonances of lysozyme in the absence and presence of tri-NAG. (a) Lysozyme. (b) Same as (a) with 10 mM HyTEMPO added. (c) Same as (a) with 10 mM tri-NAG added. (d) Same as (a) with 10 mM tri-NAG and 10 mM HyTEMPO added.

for 12 of the 14 residues examined, including Asp and Gly residues. One exception is Val 109, which has exposure to the probe in the crystal structure but is less broadened than might be expected. The other is Ile 98. Ile 98 is very sensitive to nitroxyl but has no area accessible to the 2.5-Å probe of the crystal structure; it is exposed to a 1.4-Å probe, however (Lee & Richards, 1971).

Hen egg white lysozyme binds tri-*N*-acetylglucosamine (tri-NAG) with a dissociation constant of 6.6×10^{-6} M (Dahlquist et al., 1966). We examined the effect of HyTEMPO on side-chain resonances near the substrate binding site in the presence and in the absence of this inhibitor. Panels c and d of Figure 8 illustrate, for example, that the $C^{\gamma}H$–$C^{\delta}H_3$ peak of Leu 75, which is part of the binding site, although broadened somewhat by association with tri-NAG, is protected by the ligand from the nitroxyl. Panels c and d of Figure 9 show similarly that the Ala 107 resonance is shifted and

broadened by tri-NAG but protected by it from nitroxyl. In these experiments, enzyme concentration was 5 mM and inhibitor concentration 10 mM, so that complex formation was nearly complete. Titration of lysozyme with tri-NAG showed that on the chemical shift time scale the inhibitor exchanges at an intermediate to slow rate, as monitored by following the behavior of the Trp 62 H^2 singlet. This is consistent with the reported k_{off} rate of 28 s^{-1} (Chipman & Schimmel, 1968).

Further results of the lysozyme and lysozyme plus inhibitor experiments are reported elsewhere (Petros & Kopple, 1990) and indicate that the effects of nitroxyl can indeed be used to identify residues in the inhibitor binding region; i.e., residues exposed to HyTEMPO in the absence of tri-NAG become less exposed in its presence. The technique is thus an alternative to the use of spin-labeled ligand as proposed by deJong et al. (1988). Those experiments and the above results do indicate the utility of nitroxyl-catalyzed relaxation in DQF-COSY spectra as a probe of exposed hydrophobic residues and ligand binding sites including them.

ACKNOWLEDGMENTS

We thank Dr. Robert E. Rycyna for preparation of the Gd[DTPA] used in these studies, Dr. Paul L. Weber for helpful discussions, and Dr. Charles Hutchins, Abbott Laboratories, for help in generating the stereo drawing of Figure 7.

REFERENCES

Blake, C. C. F.; Koenig, D. F., Mair, G. A., North, A. C. T., Phillips, D. C., & Sarman, V. R. (1965) *Nature 206*, 757–760.

Chazin, W. J., Rance, M., & Wright, P. E. (1987) *FEBS Lett. 232*, 109–114.

Chipman, D. M., & Schimmel, P. R. (1968) *J. Biol. Chem. 243*, 3771–3774.

Connolly, M. L. (1981) *Science 221*, 707–713.

Dahlquist, F. W., Jao, L., & Raftery, M. (1966) *Proc. Natl. Acad. Sci. U.S.A. 56*, 26–35.

deJong, E. A. M., Claesen, C. A. A., Daemen, C. J. M., Harmsen, B. J. M., Konings, R. N. H., Tesser, G. I., & Hilbers, C. W. (1988) *J. Magn. Reson. 80*, 197–213.

Diamond, R. (1974) *J. Mol. Biol. 82*, 371–391.

DiStephano, D. L., & Wand, A. J. (1987) *Biochemistry 26*, 7272–7281.

Jabusch, J. R., & Deutsch, H. F. (1985) *Arch. Biochem. Biophys. 238*, 170–177.

Jenkins, B. G., & Lauffer, R. B. (1978) *Inorg. Chem. 27*, 4730–4738.

Kaptein, R. (1982) *Biol. Magn. Reson. 4*, 145–191.

Kaptein, R., Dijkstra, K., & Nicolay, K. (1978) *Nature 274*, 293–294.

Kemple, M. D., Ray, B. D., Lipkowitz, K. B., Prendergast, F. G., & Nageswara Rao, B. D. (1988) *J. Am. Chem. Soc. 110*, 8275–8287.

Kopple, K. D., & Schamper, T. J. (1972) *J. Am. Chem. Soc. 94*, 3644–3646.

Kopple, K. D., & Zhu, P. P. (1983) *J. Am. Chem. Soc. 105*, 7742–7746.

Kopple, K. D., Ohnishi, M., & Go, A. (1969) *J. Am. Chem. Soc. 91*, 4264–4272.

Kosen, P. A., Scheek, R. M., Naderi, H., Basus, V. J., Manogaran, S., Schmidt, P. G., Oppenheimer, N. J., & Kuntz, I. D. (1986) *Biochemistry 25*, 2356–2363.

Lane, A. N., & Jardetzky, O. (1985) *Eur. J. Biochem. 152*, 411–418.

Lee, B., & Richards, F. M. (1971) *J. Mol. Biol. 55*, 379–400.

Marsh, J. K. (1955) *J. Chem. Soc. Part 1*, 451–452.

Molday, R. S., Englander, S. W., & Kallen, R. G. (1970) *Biochemistry 11*, 150–158.

Morishima, I., Ishihara, K., Tomishima, K., Inubushi, T., & Yonezawa, T. (1975) *J. Am. Chem. Soc. 97*, 2749–2756.

Niccolai, N., Valensin, G., Rossi, C., & Gibbons, W. A. (1982) *J. Am. Chem. Soc. 104*, 1534–1537.

Petros, A. M., & Kopple, K. D. (1990) *Biochem. Pharmacol. 40*, 65–68.

Phillips, D. C. (1967) *Proc. Natl. Acad. Sci. U.S.A. 57*, 484–495.

Piantini, U., Sorensen, O. W., & Ernst, R. R. (1982) *J. Am. Chem. Soc. 104*, 6800–6801.

Pitner, T. P., Glickson, J. D., Rowan, R., Dadok, J., & Bothner-By, A. A. (1975) *J. Am. Chem. Soc. 97*, 5917–5918.

Redfield, C., & Dobson, C. M. (1988) *Biochemistry 27*, 122–136.

Rubin, M., & Dexter, M. (1982) U.S. Patent 3,062,719 (Geigy Chemical Corp.).

Shaka, A. J., & Freeman, R. (1983) *J. Magn. Reson. 51*, 169–173.

States, D. J., Haberkorn, R. A., & Ruben, D. J. (1982) *J. Magn. Reson. 48*, 286–292.

Stezowski, J. J., & Hoard, J. L. (1984) *Isr. J. Chem. 24*, 323–334.

Stob, S., Sheek, R. M., Boelens, R., Dijkstra, K., & Kaptein, R. (1988) *Isr. J. Chem. 28*, 319–327.

Vijay-Kumar, S., Bugg, C. E., & Cook, W. J. (1987) *J. Mol. Biol. 194*, 531–544.

Wagner, G., & Wuthrich, K. (1982) *J. Mol. Biol. 160*, 343–361.

Weber, P. L., Brown, S. C., & Mueller, L. (1987) *Biochemistry 26*, 7282–7290.

Weiss, M. A., Eliason, J. L., & States, D. J. (1984) *Proc. Natl. Acad. Sci. U.S.A. 81*, 6019–6023.